

Supplemental material

Fluorite $\text{TiO}_2(111)$ Surface Phase for Enhanced Visible-Light Solar Energy

Conversion

State Key Laboratory of Organic-Inorganic Composites,

Beijing University of Chemical Technology, Beijing 100029, China

Mang Niu, Daojian Cheng, and Dapeng Cao

1. Atomic structures of high-pressure TiO_2 phases.

The atomic structure of the baddeleyite, columbite, orthorhombic, cotunnite, pyrite, and fluorite TiO_2 are displayed in Figure S1.

2. Total and partial density of states of high-pressure TiO_2 phases.

To further understand the band gap reduction in fluorite TiO_2 , the density of states (DOSs) for of baddeleyite, columbite, orthorhombic, cotunnite, pyrite, and fluorite TiO_2 were calculated, as shown in Figure S2. For all these systems, the valence band (VB) of high-pressure phase of TiO_2 consists mainly of the O-2p states, whereas the conduction band (CB) is dominated by the Ti-3d states. It is found that the Ti-3d states in the CB of cubic fluorite TiO_2 split into e_g and t_{2g} states.

3. Optical absorption properties of fluorite and rutile TiO₂.

The optical absorption property of fluorite TiO₂ has been evaluated through the frequency-dependent imaginary part of the dielectric tensor $\varepsilon_2(\omega)$ and the corresponding result of rutile TiO₂ is also displayed in Figure S2 for comparison. The results indicate that the fluorite TiO₂ is visible-light active due to its reduced band gap.

4. Slab models of rutile TiO₂(110), rutile TiO₂(011), pyrite TiO₂(111), and fluorite TiO₂(111) surfaces.

The TiO₂ surfaces were modeled by the periodic slabs with a vacuum region of 10 Å to minimize the interactions between the neighboring atomic layers. The top and side views of the four-layer slabs for rutile TiO₂(110), rutile TiO₂(011), pyrite TiO₂(111), and fluorite TiO₂(111) surfaces were displayed in Figure S4. For the geometry optimization, a 5×5×1 *k*-point mesh was used and all the atoms were allowed to relax. The surface energy is defined as:

$$E_{surf} = \frac{E_{slab} - NE_{bulk}}{2A}, \quad (1)$$

Where E_{slab} is the total energy of slab. E_{bulk} is the total energy of per repeating cell of bulk crystal and the slab containing N repeating cell. A is the surface area of the slab.

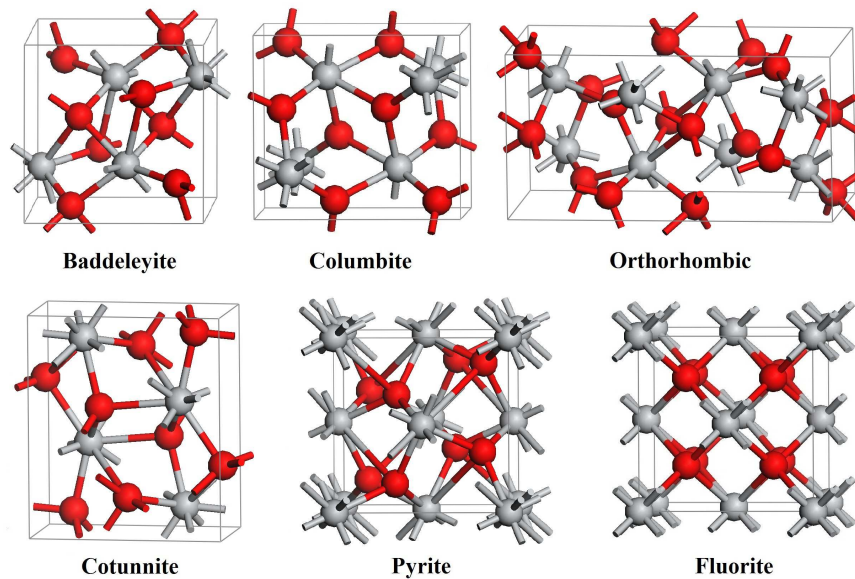


Figure S1. Atomic structures of baddeleyite, columbite, orthorhombic, cotunnite, pyrite, and fluorite TiO_2 crystals. The gray and red spheres represent the Ti and O atoms, respectively.

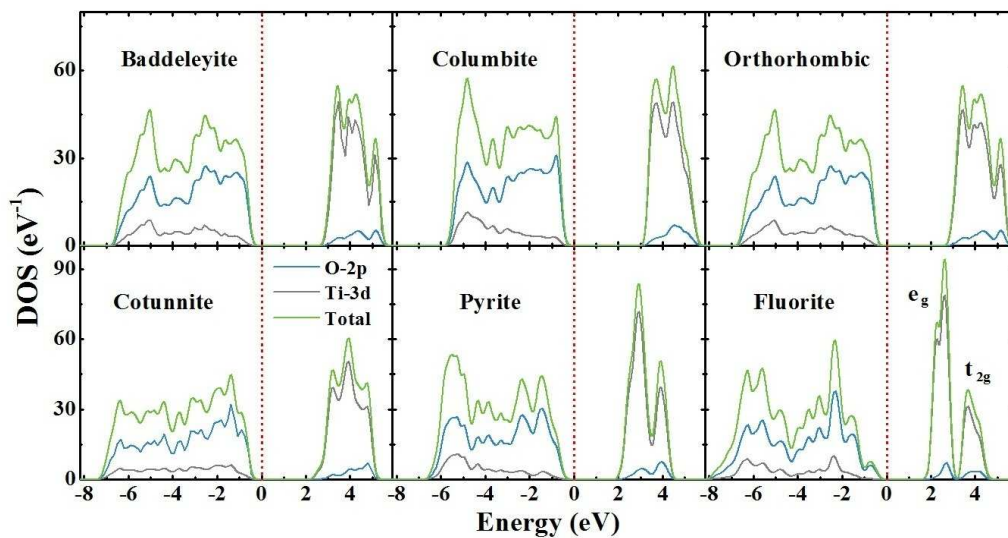


Figure S2. HSE06 calculated total and partial DOSs of baddeleyite, columbite, orthorhombic, cotunnite, pyrite, and fluorite TiO_2 . The Fermi level of these high-pressure phases of TiO_2 is displayed with a red dashed line.

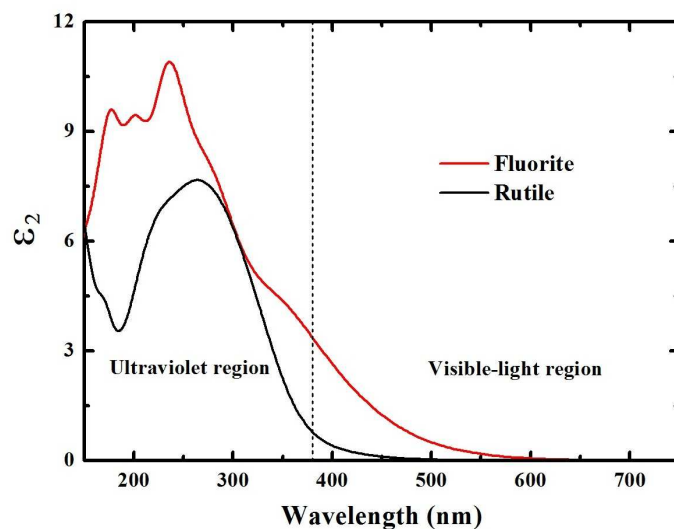


Figure S3. The imaginary part of the dielectric function (ϵ_2) for bulk rutile and fluorite TiO_2 , calculated with HSE06 functional. The present data were averaged over the three (x , y , and z) polarization vectors.

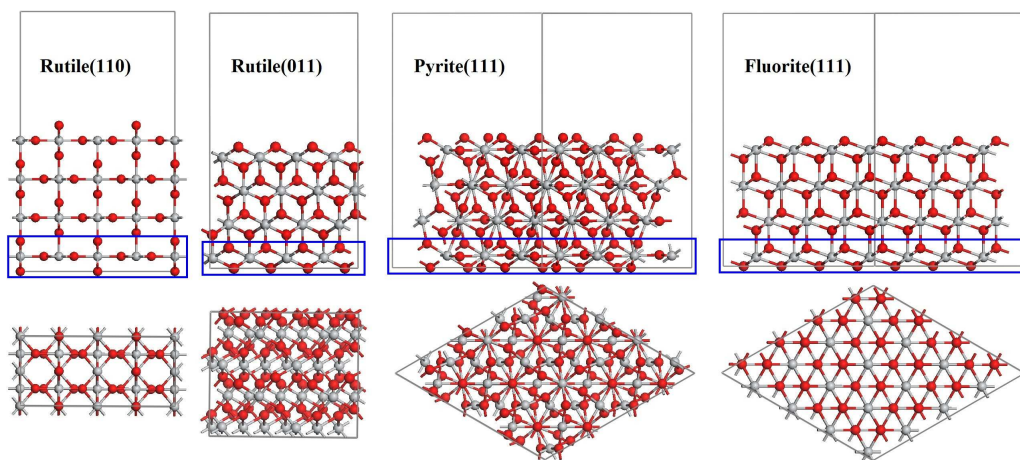


Figure S4. The side and top views of the four-layer slabs for rutile $\text{TiO}_2(110)$, rutile $\text{TiO}_2(011)$, pyrite $\text{TiO}_2(111)$, and fluorite $\text{TiO}_2(111)$ surfaces. The gray and red spheres represent the Ti and O atoms, respectively. The repeat unit layer of these TiO_2 slabs is illustrated in the blue rectangle. A vacuum region of 10\AA was used in these slab models.